

Open-Ended 3D Point Cloud Instance Segmentation

Phuc Nguyen^{1*} Minh Luu^{1*} Anh Tran¹ Cuong Pham^{1,2} Khoi Nguyen¹
¹VinAI Research ²Posts & Telecommunications Inst. of Tech

Abstract

Open-Vocab 3D Instance Segmentation methods (OV-3DIS) have recently demonstrated their ability to generalize to unseen objects. However, these methods still depend on predefined class names during testing, restricting the autonomy of agents. To mitigate this constraint, we propose a novel problem termed **Open-Ended 3D Instance Segmentation (OE-3DIS)**, which eliminates the necessity for predefined class names during testing. Moreover, we contribute a comprehensive set of strong baselines, derived from OV-3DIS approaches and leveraging 2D Multimodal Large Language Models. To assess the performance of our OE-3DIS system, we introduce a novel Open-Ended score, evaluating both the semantic and geometric quality of predicted masks and their associated class names, alongside the standard AP score. Our approach demonstrates significant performance improvements over the baselines on the ScanNet200 and ScanNet++ datasets. Remarkably, our method surpasses the performance of Open3DIS, the current state-of-the-art method in OV-3DIS, even in the absence of ground-truth object class names.

1 Introduction

3D point cloud instance segmentation (3DIS) [1, 2, 3, 4, 5, 6], also known as closed-vocabulary 3D instance segmentation, aims to segment all points in a point cloud into instances of classes predefined in the training set. However, this approach is less practical for scenarios where the test classes are unknown or different from the training classes. This limitation has led to the development of open-vocabulary 3D instance segmentation (OV-3DIS) [7, 8, 9, 10, 11, 12]. Despite these advancements, OV-3DIS methods face several practical challenges. One major challenge is that class names must be predefined during testing, necessitating human intervention for scene understanding. This requirement significantly impedes the perception of truly autonomous agents. A potential solution is to predefined large and comprehensive vocabularies; however, this can lead to inaccuracies and significantly degrade the performance of OV-3DIS when an excessive number of vocabularies are used.

To overcome these limitations, we introduce a novel task called **Open-Ended 3D Point Cloud Instance Segmentation (OE-3DIS)**. Unlike traditional methods, OE-3DIS does not require predefined class names during testing. Given a 3D point cloud and RGBD sequence, the system automatically generates a set of 3D masks along with their class names. To evaluate the performance of OE-3DIS methods, we propose a new metric called the OE score, in addition to the standard AP score. The OE score measures both the intersection-over-union (IoU) of the predicted instance masks with the ground-truth masks and the semantic similarity between the predicted and ground-truth class names.

To address this new and challenging task, we investigate several typical approaches: leveraging OV-3DIS methods and utilizing Multimodal Large Language Models (MLLMs). In the first approach, a list of class names is either predefined from large vocabularies or pre-extracted from image taggers. In the second approach, 2D visual tokens extracted from a pretrained 2D CLIP encoder are lifted to 3D and used as 3D visual token inputs to an LLM to predict class names. Among these methods, we find that pointwise visual token lifting to 3D for use as input to the LLM performs the best and

*These authors contributed equally to this work

is selected as our chosen approach. This method performs on par with state-of-the-art OV-3DIS approaches, where ground-truth classes are provided. Additionally, this approach is training-free, leveraging a pretrained 2D vision encoder (e.g., CLIP [13]) and a pretrained LLM (e.g., Vicuna [14]), thereby mitigating the drawback of limited training data faced by many 3D-LLM methods.

To evaluate the performance of these methodologies, we conduct experiments on open-ended versions of two prominent 3D instance segmentation (3DIS) datasets: ScanNet200 [15] and ScanNet++ [16]. The results underscore the efficacy of our chosen approach over alternative baselines, demonstrating performance levels comparable to OV-3DIS methods that rely on ground-truth class names. Specifically, in ScanNet200, our approach attained an AP of 16.0, contrasting with the 22.2 AP achieved by Open3DIS, currently recognized as the state-of-the-art in OV-3DIS. However, our approach is superior in ScanNet++, where it outperforms Open3DIS by a significant margin (18.4 vs. 13.1).

In summary, the contributions of our work are:

1. We propose Open-Ended 3D Point Cloud Instance Segmentation (OE-3DIS), a task that segments 3D point clouds by instances and generates class names without predefined labels.
2. We introduce the OE score, which evaluates both the IoU of predicted instance masks with ground-truth masks and the semantic similarity of predicted and ground-truth class names.
3. We explore approaches for OE-3DIS, including leveraging OV-3DIS methods and Multi-modal Large Language Models (MLLMs).
4. We present a training-free OE-3DIS method that lifts 2D visual tokens to 3D for LLM input, utilizing pretrained models like EVA-CLIP and Vicuna. This approach outperforms other baselines and achieves performance comparable to OV-3DIS methods using ground-truth class names on ScanNet200 and ScanNet++ benchmarks.

2 Related Work

3D instance segmentation (3DIS) methods such as Mask3D [2], ISNet [3], PointGroup [6], and others [17, 18, 19, 20] cluster a point cloud scene into 3D instance masks of classes predefined in the training set. These methods utilize a 3D Convolutional backbone [21, 22, 23] to extract semantic information from the 3D scene. Subsequently, they employ either Dynamic Convolution-based [4] or Grouping-based [5] modules to generate 3D instance masks. Recently, some approaches have adopted techniques to back-project 2D information aggregated from multiple views onto the 3D point cloud to create an ensemble of 3D point cloud features [24, 12, 25, 26]. These 2D-derived features contain rich semantic information, while those derived from 3D capture the geometrical structure of 3D objects. Combined, they supervise a 3D instance decoder to refine segmentation masks. However, these methods are closed-vocab or cannot segment new classes in testing, limiting the capability of agents to understand new 3D scenes.

Open-vocabulary 3D instance segmentation (OV-3DIS) aims at segmenting 3D objects of classes newly provided in testing. To provide 3D proposals for object recognition, OpenMask3D [8] and Lowis3D [27] employ 3DIS networks [3, 2] to generate class-agnostic 3D proposals, while SAI3D [10], MaskClustering [11], and OVIR [9] utilize 2D segmenter for producing masks for each view and consistently lift these masks to 3D. While 3DIS networks excel in capturing large geometrical structures, they often struggle to detect rare and small-shaped objects. Conversely, 2D segmenters are adept at focusing on small regions but face challenges in maintaining object consistency when lifting to the 3D point cloud. Open3DIS [7] addresses these limitations by combining both 3D and 2D branches, resulting in superior results. This approach effectively captures rare and small objects while preserving the 3D geometrical structures of large objects using superpoint-level masks. While OV-3DIS is useful in some scenarios, the constraint of a predefined vocabulary set in testing requires human intervention, hindering truly autonomous agents.

3D scene understanding with Large Language Models (LLMs). Utilizing LLMs for 3D scene understanding focuses on how objects are aligned, their directions, and their locations based on textual questions within 3D environments. This approach emphasizes the spatial aspects of language understanding in three dimensions of data. Previous works [28, 29, 30, 31, 32] have contributed to providing 3D spatial data with language for various applications, including 3D instance and scene

captioning [33, 34, 35, 36, 29, 37, 28], 3D visual answering questions [29, 30, 38, 39, 37, 28, 40, 33], 3D visual grounding [37, 28, 29, 31, 32, 41] and supporting embodied AI tasks like planning and reasoning [28, 37, 29, 33].

Open-ended 2D Image Understanding is an emerging task that addresses the need to recognize objects without predefined class names during training or testing. There is scant work on this task, with existing research primarily focusing on image classification [42, 43, 44], object detection [45], and instance segmentation [46, 47, 48]. Standard 2D Multimodal LLMs (2D MLLMs), such as LLAVA [49], consist of a frozen vision encoder, a projector, and an LLM module. These models typically finetune either (1) the linear projector and the LLM or (2) a complex Q-Former projector. However, applying these methods for 3D scene understanding (3D-LLMs) is challenging due to the lack of sufficient 3D data and text description pairs to effectively train 3D-LLMs. In this paper, we present a novel approach to leveraging pretrained 2D MLLMs for OE-3DIS.

OmniScient Model (OSM) [47] is a recently proposed pretrained 2D Multimodal LLM for Open-ended 2D Instance Segmentation, which serves as the foundation for our proposed method. OSM comprises three main modules: a visual encoder, a MaskQ-Former, and a Large Language Model (LLM). The visual encoder is a pretrained EVA-CLIP [50], a variant of the CLIP model [13], which extracts high-resolution visual features using a sliding-window scheme and incorporates global positional embeddings to preserve spatial information. The MaskQ-Former, a customized version of Q-Former [51] designed to focus on the mask region rather than the entire image, converts visual features into fixed-length visual tokens. These tokens are then input into the Vicuna LLM [14]. The LLM processes these tokens to answer the question, “What is in the segmentation mask?” by outputting the object name.

In OSM, only the MaskQ-Former is trained to align visual features with the visual tokens for the LLM, while the visual encoder and LLM remain unchanged. The training datasets are large, including COCO [52], LVIS [53], ADE20K [54], and Cityscapes [55]. This setup demonstrates a strong capability for recognizing objects without predefined class names in 2D images, inspiring us to extend this approach to 3D scene understanding.

3 Methodology

3.1 Problem Statement

Given a 3D point cloud scene $\mathbf{P} = \{\mathbf{p}_i\}_{i=1}^N \in \mathbb{R}^{N \times 6}$ consisting of N points with xyz coordinates and associated rgb colors, along with T RGB-D frames with color images $\{\mathbf{I}_t\}_{t=1}^T$ and depth ones $\{\mathbf{D}_t\}_{t=1}^T$, where $\mathbf{I}_t \in \mathbb{R}^{H \times W \times 3}$, $\mathbf{D}_t \in \mathbb{R}_+^{H \times W}$, we aim to segment all K object binary masks $\{\mathbf{m}_k\}_{k=1}^K$, $\mathbf{m}_k \in \{0, 1\}^N$ and their associated class names $\{l_k\}_{k=1}^K$ without giving any predefined class names in testing.

The auxiliary information includes the intrinsic matrix $\mathbf{\Gamma} \in \mathbb{R}^{3 \times 3}$ and the extrinsic matrix $[\mathbf{R}|\mathbf{v}]_t \in \mathbb{R}^{3 \times 4}$, where H, W are the image’s height and width, \mathbf{R} is a 3D rotation matrix, and \mathbf{v} is a 3D translation vector. This composite matrix of rotation and translation converts coordinates from the global frame (of the point cloud) to the camera’s frame at view t .

3.2 Evaluation Metrics

To evaluate open-ended object detection or instance segmentation, where predicted class names may be similar but not exactly the same as ground-truth (GT) class names, prior work [56] proposed a label reassignment technique. This method uses text encoders (e.g., CLIP [13], BERT [57], Sentence Transformer [58]) to encode both the predicted and GT class names for each scene. It then matches each predicted class name to its closest GT class name based on cosine similarity. After this matching, the standard **AP score** is used to evaluate performance.

However, the AP score described above is based on a many-to-one matching where multiple predicted class names can be matched to the same ground-truth class name, leading to inaccuracies in fine-grained class prediction. To address this, we propose a new metric called the **Open-ended score (OE score)**, which considers both textual semantic similarity and spatial similarity of predicted and ground-truth masks and their class names. Specifically, given K predicted instances with masks,

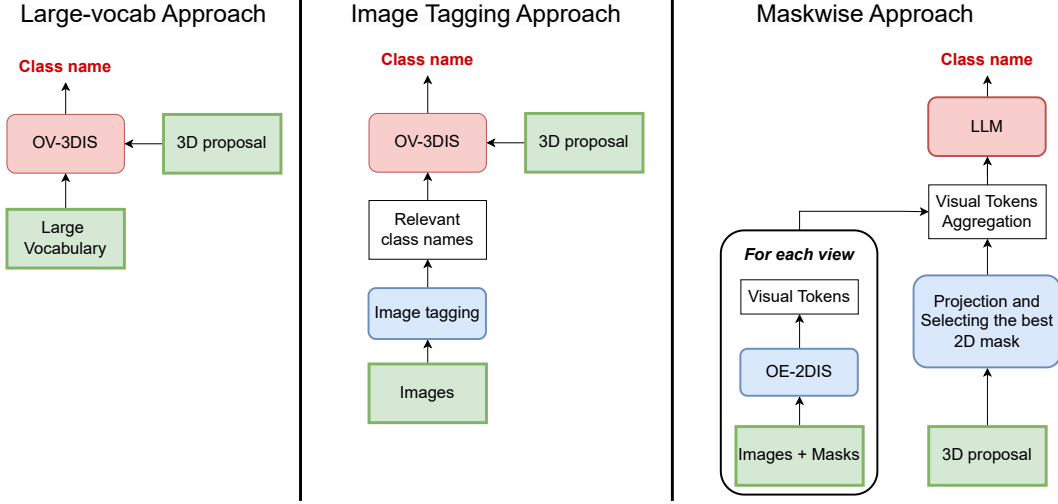


Figure 1: Our baselines: Large-vocab (Left), Image tagging (Middle), and Maskwise (Right).

class names, and confidence scores $\{\mathbf{m}_k\}_{k=1}^K$, $\{l_k\}_{k=1}^K$, and $\{\rho_k\}_{k=1}^K$, and J ground-truth instances with masks and class names as $\{\mathbf{m}_j\}_{j=1}^J$ and $\{l_j\}_{j=1}^J$, we first compute the cosine similarity $s_{k,j}$ between the text embeddings of the predicted and ground-truth class names, along with the IoU $o_{k,j}$ between predicted and ground-truth masks. Next, we construct the cost matrix $\mathbf{C} \in [0, 1]^{K \times J}$ for one-to-one Hungarian matching as follows:

$$\mathbf{C}(k, j) = -\sqrt[3]{o_{k,j} \cdot \rho_k \cdot \max(0, s_{k,j})}. \quad (1)$$

In this way, only the best-matched 3D predictions in both text and mask are considered for evaluation. The final OE score is obtained by averaging all costs of matched pairs, or

$$\text{OE score} = 100 * \frac{\sum_{(k,j) \in \text{all matched pairs}} -\mathbf{C}(k, j)}{J}. \quad (2)$$

We average over J GT masks since the number of GT masks is always smaller than the number of predicted masks.

3.3 Proposed Baselines

Since OE-3DIS is very new and challenging, even more so than OV-3DIS, we focus our efforts on investigating prominent baselines. These baselines are illustrated in Fig. 1. They require a list of class-agnostic 3D mask proposals pre-extracted from Open3DIS [7] with the DETIC 2D segmenter.

Large-vocab approach (Fig. 1 - Left): We start with a simple OE-3DIS baseline by using a large vocabulary of 21K common classes introduced by DETIC [59] as predefined class names for OV-3DIS methods like Open3DIS [7] and OpenMask3D [8]. However, this approach fails to achieve robust class prediction. This is because the fixed large vocabulary set contains multiple synonyms, resulting in uninformative class predictions after the Softmax operation.

Image Tagging approach (Fig. 1 - Middle): To reduce the number of classes, we leverage image-tagging techniques such as RAM++ [44] to obtain only relevant class names per scene. Specifically, for each input view, a set of image tags is generated and then combined across all processed input views. The resulting unified tag set serves as the vocabulary for OV-3DIS. However, these methods often produce inconsistent class names across views, leading to redundant and similar class names.

Maskwise approach (Fig. 1 - Right): To tackle the inconsistency in class names across views, we first apply an OE-2DIS method, such as OSM [47], to each view to obtain a list of 2D masks and their predicted fixed-length visual tokens. For each 3D mask proposal, we project it onto a view and

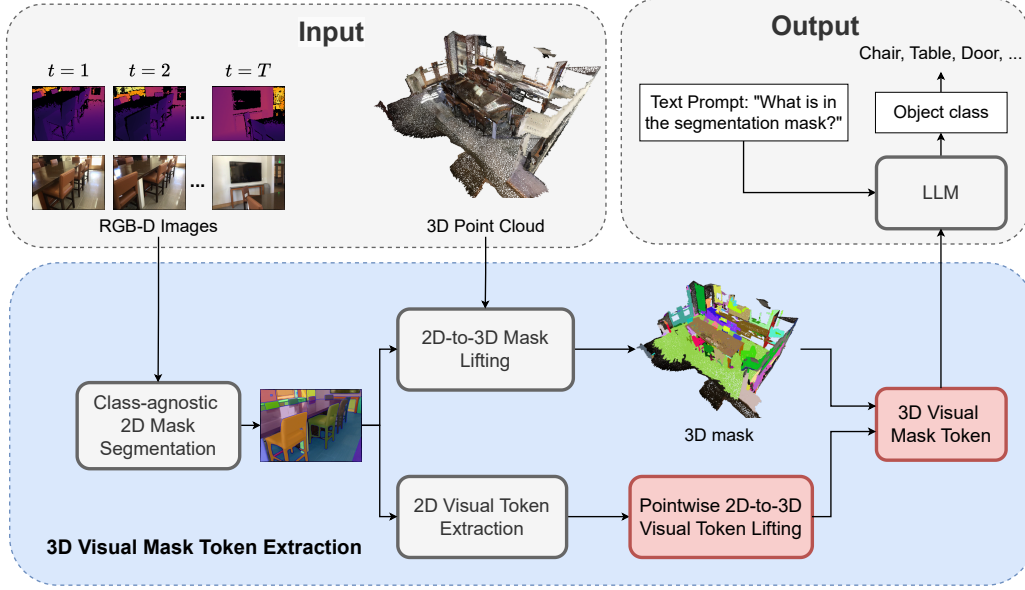


Figure 2: **Overview of our approach.** First, we generate class-agnostic 2D instance segmentation masks for all views using segmenters like DETIC [59] and SAM [60], and lift these 2D masks into 3D masks using Open3DIS [7]. Simultaneously, the 2D masks and their corresponding RGB images are used to extract 2D visual tokens from an MLLM like OSM [47], which are then lifted into pointwise 3D visual tokens. Finally, for each 3D proposal mask, we aggregate the pointwise 3D visual tokens to form the final tokens for input to the LLM to predict final class names.

associate it with the best-matched 2D mask based on IoU to obtain its 2D fixed-length visual tokens. The 3D visual tokens for the 3D mask are then aggregated by averaging the 2D visual tokens across views, which are subsequently input into a pretrained LLM to obtain the final class names. However, this approach heavily relies on the matching process between the 3D proposal and 2D masks in each view, which is often misaligned due to imperfect segmentation and depth maps. In other words, a 3D mask can project onto multiple 2D masks, and selecting only the best-matched 2D mask might result in the loss of important information.

3.4 Our Approach

To address the above limitations, we propose a method for producing pointwise 3D visual tokens, as illustrated in Fig. 2. First, we generate class-agnostic 2D instance segmentation masks for all views using class-agnostic 2D segmenters such as DETIC [59] and SAM [60]. Next, we lift 2D masks into 3D masks using Open3DIS [7]. Simultaneously, these 2D masks, along with their corresponding RGB images, are used to extract 2D visual tokens from an MLLM like OSM [47]. We then lift the resulting 2D visual tokens \mathbf{F}^{2D} into 3D visual tokens to obtain pointwise 3D visual tokens \mathbf{F}^{3D} . Finally, for each 3D proposal mask, we query the 3D visual tokens associated with this proposal by aggregating the pointwise lifted 3D visual tokens, forming the final tokens \mathbf{f}^{3D} for input to the LLM.

This approach takes into account the depth and geometric structure of 3D objects via lifting, resulting in more robust visual tokens and a unified, densely-featured point cloud that can be queried instantly at test time. Subsequently, we will focus on our pointwise visual tokens lifting and aggregation.

First, the correspondence of a 3D point $\mathbf{p}_i(x, y, z) \in \mathbf{P}$ with its 2D projection (u, v) in view t is:

$$d_{i,t} \cdot \begin{bmatrix} u_i \\ v_i \\ 1 \end{bmatrix}_t = \mathbf{\Gamma} \cdot [\mathbf{R}|\mathbf{c}]_t \cdot \begin{bmatrix} x_i \\ y_i \\ z_i \\ 1 \end{bmatrix} \quad (3)$$

where $d_{i,t}$ is the projected 2D depth value of point i to frame t .

For each view t , we extract the 2D visual tokens $\mathbf{F}_t^{k,2D} \in \mathbb{R}^{E \times C}$, where E, C are the number of visual tokens and feature dimensions, for each 2D mask k from the MaskQ-Former module of OSM [47]. Furthermore, we denote $\lambda_{t,i}^k = \{0, 1\}$ as the visibility value indicating a point i is visible in mask k of view t , $\lambda_t^k = \{0, 1\}^N$. We set the visibility value $\lambda_{t,i}^k$ of any points whose pixel projections fall outside the k -th 2D mask’s boundaries or the disparity between projected depth d and the collected depth \mathbf{D} exceeds a defined depth threshold τ_{depth} , or $|d_{i,t} - \mathbf{D}_t[\lfloor u_i \rfloor, \lfloor v_i \rfloor]| > \tau_{\text{depth}}$, to 0.

We accumulate 3D visual tokens $\mathbf{F}^{3D} \in \mathbb{R}^{N \times E \times C}$, from every 2D mask k and compute for the frequency $\mathbf{r}^{3D} \in \mathbb{N}^N$ of every view as follows:

$$\mathbf{F}^{3D} = \sum_{t,k} \lambda_t^k * \mathbf{F}_t^{k,2D}, \quad \mathbf{r}^{3D} = \sum_{t,k} \lambda_t^k, \quad (4)$$

where $*$ is the outer product. The normalized pointwise 3D visual tokens are then obtained as follows:

$$\bar{\mathbf{F}}_i^{3D} = \begin{cases} \mathbf{F}_i^{3D} / \mathbf{r}_i^{3D} & \text{if } \mathbf{r}_i^{3D} > 0 \\ \mathbf{0} & \text{otherwise} \end{cases}. \quad (5)$$

Finally, for each 3D mask \mathbf{m}_k , we weighted average the visual tokens of all its points by their frequency to obtain the 3D visual tokens \mathbf{f}_k^{3D} for that mask, which are then used as input to the LLM to predict the final class, as follows.

$$\mathbf{f}_k^{3D} = \frac{\sum_{i \in \mathbf{m}_k} \bar{\mathbf{F}}_i^{3D} \cdot \mathbf{r}_i^{3D}}{\sum_{i \in \mathbf{m}_k} \mathbf{r}_i^{3D}}. \quad (6)$$

4 Experimental Results

Datasets: We conducted experiments to assess the performance of the baselines and our proposed method using two common 3DIS datasets: ScanNet200 [15] and ScanNet++ [16]. The *ScanNet200* dataset builds on the original ScanNet [61] by expanding its semantic categories from 20 to 200. Its instance segmentation benchmark includes 1,201 training scenes and 312 validation scenes with 198 object categories, significantly enriching the vocabulary and enhancing its capability for detailed 3D semantic and instance segmentation. The *ScanNet++* dataset was recently introduced, featuring up to 1,659 semantic categories, with 360 training scenes and 50 validation scenes. Given the large number of classes, we follow the standard 3DIS evaluation protocol on ScanNet++ and evaluate only the most common 100 object categories. This dataset offers a much denser 3D point cloud scene representation, making it the most challenging dataset for 3D understanding.

Evaluation metrics: We assess OE-3DIS using two metrics: the label reassignment AP score (detailed in Sec. 3.2) and our newly proposed OE score. For ScanNet200, we also report AP_{head} , AP_{com} , and AP_{tail} . For ScanNet++, we include the recall rate (RC) and average recall rate (AR). We note that the OV-3DIS methods adopt a specific AP score calculation protocol by assigning a confidence score of 1.0 to each 3D proposal. Similarly, we follow the same evaluation protocol as the Fully-sup 3DIS by ranking 3D proposals according to their confidence scores. In the context of OE-3DIS, our approach utilizes the confidence scores generated by the LLM, while potential baselines employ the CLIP score.

Implementation details: Following Open3DIS [7], we generate class-agnostic 3D proposals from ISNet [3] pretrained on ScanNet200 or by lifting 2D masks to 3D using Detic [59]. For RAM++ [44], we employ the Swin-L model, trained on a 14-million image dataset with an image size of 384px and a tagging threshold of 0.68. For LLM, we leverage Vicuna-7B [62], fine-tuned for open-ended 2D Instance Segmentation [47].

4.1 Comparison with Baselines

We compare our approach to the proposed baselines using the OE-3DIS setting on the ScanNet200 (Tab. 1) and ScanNet++ (Tab. 2) datasets. For reference, we also present results from OV-3DIS methods, including OpenMask3D [8] and Open3DIS [7], as well as fully-supervised methods like ISNet [3] and Mask3D [2] for ScanNet200; and PointGroup [6] and SoftGroup [5] for ScanNet++.

Table 1: Comparative results on the ScanNet200 dataset. Shaded text indicates a reference method, not a direct comparison. ‘-’ indicates results are not provided. The best results are in **bold**.

Setting	Method	AP	AP ₅₀	AP ₂₅	AP _{head}	AP _{com}	AP _{tail}	OE
Fully-sup 3DIS	Mask3D [2]	26.9	36.2	41.4	39.8	21.7	17.9	-
	ISBNNet [3]	24.5	32.7	37.6	38.6	20.5	12.5	-
OV-3DIS	OpenMask3D [8]	15.4	19.9	23.1	17.1	14.1	14.9	-
	Open3DIS [7]	23.7	29.4	32.8	27.8	21.2	21.8	-
Large-Vocab	21K DETIC classes (Ours)	8.5	11.7	13.1	9.9	7.2	8.3	52.2
Image-Tagging	RAM++ [44] (Ours)	10.7	14.3	16.0	11.6	11.0	9.3	60.5
Maskwise	OSM [47] (Ours)	14.4	19.8	23.9	18.9	13.5	10.2	65.0
Pointwise	Ours	16.0	22.0	24.7	20.0	14.3	13.2	65.2

Table 2: Comparative results on the ScanNet++ dataset. Shaded text indicates a reference method, not a direct comparison. ‘-’ indicates results are not provided. The best results are in **bold**.

Setting	Method	AP	AP ₅₀	AP ₂₅	AR	RC ₅₀	RC ₂₅	OE
Fully-sup 3DIS	PointGroup [6]	8.9	14.6	38.9	-	-	-	-
	SoftGroup [5]	16.7	29.7	21.0	-	-	-	-
OV-3DIS	OpenMask3D [8]	2.0	2.7	3.4	4.6	8.3	12.4	-
	Open3DIS (known classes) [7]	13.1	20.8	24.6	22.1	33.9	39.1	-
Large-Vocab	21K DETIC classes (Ours)	7.3	11.9	15.2	13.3	20.3	23.6	42.0
Image-Tagging	RAM++ [44] (Ours)	9.1	15.5	19.1	16.0	24.8	28.7	48.5
Maskwise	OSM [47] (Ours)	16.3	24.8	29.0	22.2	32.0	36.0	51.2
Pointwise	Ours	18.4	29.4	33.6	23.3	35.2	39.3	53.9

Table 3: Ablation on point aggregation techniques

Technique	AP	AP ₅₀	AP ₂₅	AP _{head}	AP _{com}	AP _{tail}	OE
Max	6.3	8.4	10.2	8.5	4.7	5.6	56.3
Random	13.2	18.9	21.6	17.7	12.3	10.0	60.4
Mean	14.5	20.1	22.6	18.2	13.1	11.2	63.1
Weighted Average	16.0	22.0	24.7	20.0	14.3	13.2	65.2

For ScanNet200: We obtain class-agnostic 3D proposals from two sources: 3D masks from a 3DIS network such as ISBNNet [3], and 2D Lift 3D masks from Open3DIS [7]. Our proposed approach outperforms other baselines in both AP and OE scores. Furthermore, the performance progression of the baselines, in the specified order, clearly justifies the motivation behind each baseline compared to its predecessor, as discussed in Sec. 3.3. Interestingly, our approach also surpasses OpenMask3D [8] (16.0 vs. 15.4 in AP), even though OpenMask3D utilizes provided class names. This indicates that, in some cases, we can achieve OV-3DIS without relying on provided class names.

For ScanNet++: Due to the extensive scale and vast array of classes in ScanNet++, the performance of 3D mask results from ISBNNet is inadequate. Consequently, we solely rely on the utilization of 2D Lift 3D masks from Open3DIS [7]. We notice a consistent trend akin to the results observed in ScanNet200. Particularly noteworthy is the significant outperformance of our approach compared to OV-3DIS methods or even fully-supervised 3DIS, as evidenced by higher AP scores. This underscores the promising application of OE-3DIS in navigating complex 3D scene structures.

Qualitative comparison: In Fig. 3, both our proposed baselines and approach effectively assign class names to 3D proposals in OE-3DIS settings. The first column of ScanNet200 qualitative results shows our architectures accurately predicting all 3D proposals. The second column highlights differences between our approach and the baselines. Our method precisely identifies the ‘painting’ object as “wall painting”, while other baselines predict less accurate object labels. In the final column, our 3D mask proposals offer more detail than ground truth, enabling predictions of classes not in ScanNet++’s vocabulary, such as “photocopier”.

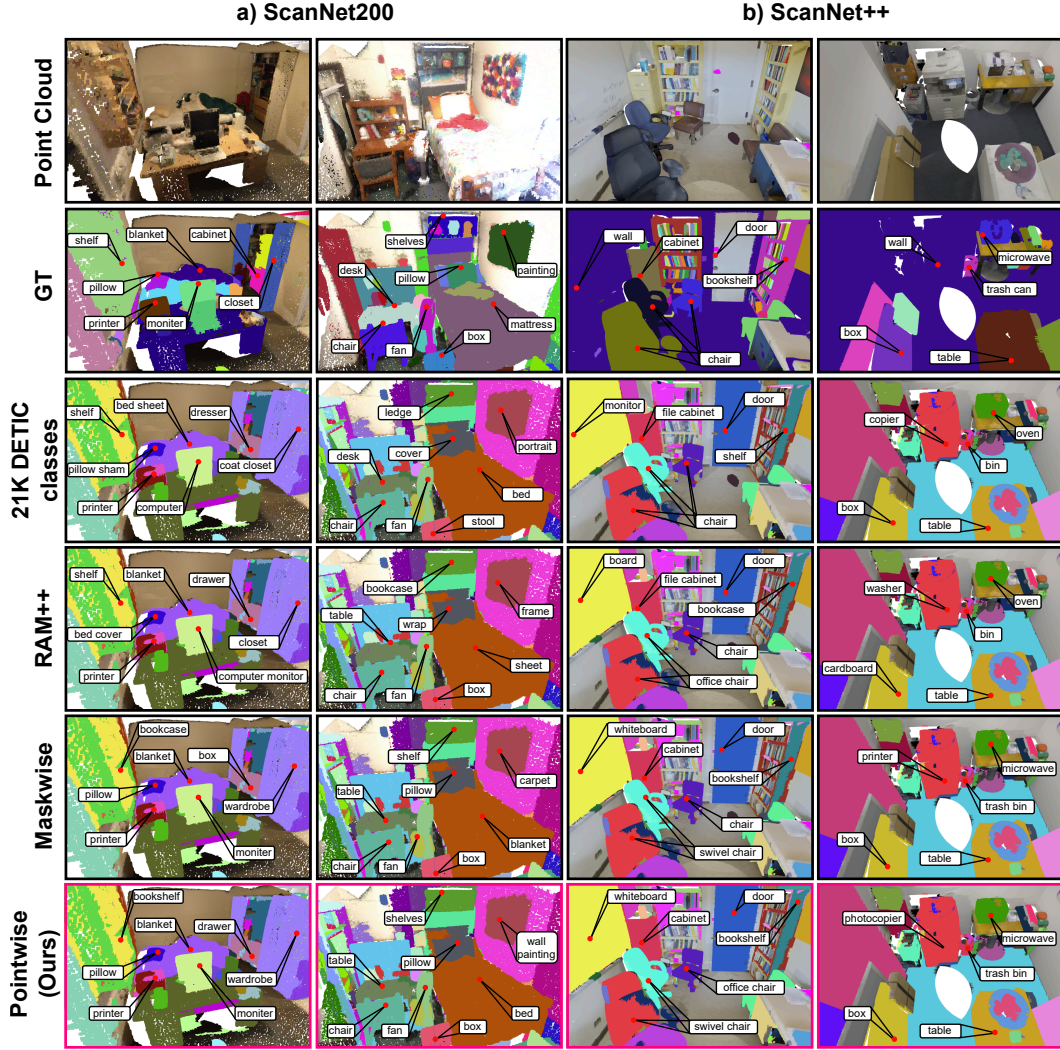


Figure 3: Qualitative examples are provided for ScanNet200 [61] (first two columns) and ScanNet++ [16] (last two columns). Both our baselines and approach yield notably good results, particularly in terms of accurately identifying class names even though they do not match exactly the GT classes.

Table 4: Study on different types 3D proposals.

3D Proposals	2D Masks	AP	AP ₅₀	AP ₂₅	AP _{head}	AP _{com}	AP _{tail}	OE
3D masks	DETIC	11.7	16.0	18.3	16.3	10.3	8.1	56.4
2D Lift 3D masks	DETIC	11.7	18.6	23.5	11.3	12.1	11.8	54.3
3D + 2D Lift 3D masks	DETIC	16.0	22.0	24.7	20.0	14.3	13.2	65.2
3D + 2D Lift 3D masks	SAM	15.4	20.5	22.9	19.2	14.8	11.7	64.8

4.2 Ablation Study

To study many design choices of our pointwise approach, we intensively carry out ablation study on the ScanNet200 [61] dataset.

Study on different point feature aggregation techniques (Eq. (6)) is shown in Tab. 3. We evaluate four techniques for combining point features from a given 3D mask: max, random (randomly selecting one point), mean, and weighted average (our proposed operation). The weighted average technique achieved the highest performance with an AP score of 16.0, outperforming the other methods. Consequently, we utilized the weighted average technique in all our experiments.

Table 5: Study on different text encoders used in evaluation metrics

Text Encoder	AP	AP ₅₀	AP ₂₅	AP _{head}	AP _{com}	AP _{tail}	OE
BERT [57]	13.5	19.0	21.2	17.6	11.6	11.0	70.6
CLIP [13]	15.9	22.0	24.5	20.3	13.7	13.3	71.6
Sentence Transformer [58]	16.0	22.0	24.7	20.0	14.3	13.2	65.2

Table 6: Study on different text prompts used to query the LLM.

Text Prompt	AP	OE
“What is in the segmentation mask? Assistant:”	16.0	65.2
“Can you describe what is in the segmentation mask region? Assistant:”	15.3	64.3
“What can you see in the segmentation mask region? Assistant:”	15.9	65.0
“Could you use a few words to describe what is in the segmentation mask region? Assistant:”	15.2	64.0
“What is this segmentation mask? Assistant:”	15.8	65.0

Study on different types 3D proposals. As reported in Tab. 4, combining 3D proposals from both 3D masks and 2D Lift 3D masks yielded the most favorable results. This outcome validates our choice of 3D proposals for the ScanNet200 dataset. Additionally, the 2D Lift 3D proposals obtained from DETIC demonstrated slightly superior performance compared to those from SAM. This observation diverges from the methodology adopted in Open3DIS [7], where provided class names are utilized to employ Grounded-SAM [63] instead of SAM [60], as in our OE-3DIS scenario.

Study on different text encoders for evaluation metrics is described in Tab. 5. We assess three text decoders: BERT [57], CLIP [13], and Sentence Transformer [58]. Among them, the Sentence Transformer embeddings attain the highest AP scores, whereas the CLIP text embeddings achieve the highest OE score. The OE score indicates that the text embeddings from CLIP exhibit a higher degree of similarity to each other, contrasting with those from the Sentence Transformer, which tend to describe complex sentences rather than solely focusing on a single class name. Hence, we lean towards selecting the Sentence Transformer as our recommended text encoder.

Study on different text prompts used to query the LLM: We experiment with various input text prompts to query the LLM for class names. Tab. 6 demonstrates that altering the prompt subtly affects the model’s accuracy. We select the prompt “What is in the segmentation mask? Assistant:” from the variants for our approach.

5 Discussion and Conclusion

Limitations: Though our method enhances open-ended 3D scene understanding, it has notable drawbacks. Firstly, it heavily relies on 2D visual tokens from the pretrained OSM, which are trained on instance segmentation datasets with limited classes. This hampers the model’s ability to recognize a wide range of classes in an open-world environment. Secondly, the performance of OE-3DIS is contingent upon class-agnostic 3D instance segmentation (3DIS) methods, which in turn rely on the quality of 3D representation and 2D-3D mapping, such as camera calibrations and depth images.

Conclusion: We have introduced Open-Ended 3D Point Cloud Instance Segmentation (OE-3DIS), which generates 3D masks and object class names without predefined labels during testing. We have explored baselines using OV-3DIS methods and MLLMs, and introduced a pointwise training-free approach leveraging OSM. We have also proposed the OE score, tailored for OE-3DIS. Experiments on ScanNet200 and ScanNet++ show our approach’s superior performance, notably outperforming Open3DIS (SOTA on OV-3DIS) on ScanNet++ without ground-truth class names.

References

- [1] Shaoyu Chen, Jiemin Fang, Qian Zhang, Wenyu Liu, and Xinggang Wang. Hierarchical aggregation for 3d instance segmentation. In *Proceedings of the IEEE/CVF International Conference on Computer Vision*, pages 15467–15476, 2021.

- [2] Jonas Schult, Francis Engelmann, Alexander Hermans, Or Litany, Siyu Tang, and Bastian Leibe. Mask3d for 3d semantic instance segmentation. In *International Conference on Robotics and Automation (ICRA)*, 2023.
- [3] Tuan Duc Ngo, Binh-Son Hua, and Khoi Nguyen. Isbnet: a 3d point cloud instance segmentation network with instance-aware sampling and box-aware dynamic convolution. In *Proceedings of the IEEE/CVF Conference on Computer Vision and Pattern Recognition*, pages 13550–13559, 2023.
- [4] Tong He, Chunhua Shen, and Anton van den Hengel. Dyco3d: Robust instance segmentation of 3d point clouds through dynamic convolution. In *Proceedings of the IEEE/CVF Conference on Computer Vision and Pattern Recognition*, pages 354–363, 2021.
- [5] Thang Vu, Kookhoi Kim, Tung M. Luu, Xuan Thanh Nguyen, and Chang D. Yoo. Softgroup for 3d instance segmentation on 3d point clouds. In *CVPR*, 2022.
- [6] Li Jiang, Hengshuang Zhao, Shaoshuai Shi, Shu Liu, Chi-Wing Fu, and Jiaya Jia. Pointgroup: Dual-set point grouping for 3d instance segmentation. In *Proceedings of the IEEE/CVF Conference on Computer Vision and Pattern Recognition*, pages 4867–4876, 2020.
- [7] Phuc D. A. Nguyen, Tuan Duc Ngo, Evangelos Kalogerakis, Chuang Gan, Anh Tran, Cuong Pham, and Khoi Nguyen. Open3dis: Open-vocabulary 3d instance segmentation with 2d mask guidance. In *Proceedings of the IEEE/CVF Conference on Computer Vision and Pattern Recognition (CVPR)*, 2024.
- [8] Ayca Takmaz, Elisabetta Fedele, Robert W. Sumner, Marc Pollefeys, Federico Tombari, and Francis Engelmann. OpenMask3D: Open-Vocabulary 3D Instance Segmentation. In *Advances in Neural Information Processing Systems (NeurIPS)*, 2023.
- [9] Shiyang Lu, Haonan Chang, Eric Pu Jing, Abdeslam Boularias, and Kostas Bekris. Ovir-3d: Open-vocabulary 3d instance retrieval without training on 3d data. In *7th Annual Conference on Robot Learning*, 2023.
- [10] Yingda Yin, Yuzheng Liu, Yang Xiao, Daniel Cohen-Or, Jingwei Huang, and Baoquan Chen. Sai3d: Segment any instance in 3d scenes. In *Proceedings of the IEEE/CVF Conference on Computer Vision and Pattern Recognition (CVPR)*, 2024.
- [11] Mi Yan, Jiazhaoh Zhang, Yan Zhu, and He Wang. Maskclustering: View consensus based mask graph clustering for open-vocabulary 3d instance segmentation. *arXiv preprint arXiv:2401.07745*, 2024.
- [12] Rui Huang, Songyou Peng, Ayca Takmaz, Federico Tombari, Marc Pollefeys, Shiji Song, Gao Huang, and Francis Engelmann. Segment3d: Learning fine-grained class-agnostic 3d segmentation without manual labels. *arXiv*, 2023.
- [13] Alec Radford, Jong Wook Kim, Chris Hallacy, Aditya Ramesh, Gabriel Goh, Sandhini Agarwal, Girish Sastry, Amanda Askell, Pamela Mishkin, Jack Clark, et al. Learning transferable visual models from natural language supervision. In *International conference on machine learning*, pages 8748–8763. PMLR, 2021.
- [14] Wei-Lin Chiang, Zhuohan Li, Zi Lin, Ying Sheng, Zhanghao Wu, Hao Zhang, Lianmin Zheng, Siyuan Zhuang, Yonghao Zhuang, Joseph E Gonzalez, et al. Vicuna: An open-source chatbot impressing gpt-4 with 90%* chatgpt quality. See <https://vicuna.lmsys.org> (accessed 14 April 2023), 2(3):6, 2023.
- [15] David Rozenberszki, Or Litany, and Angela Dai. Language-grounded indoor 3d semantic segmentation in the wild. In *Proceedings of the European Conference on Computer Vision (ECCV)*, 2022.
- [16] Chandan Yeshwanth, Yuch-Cheng Liu, Matthias Nießner, and Angela Dai. Scannet++: A high-fidelity dataset of 3d indoor scenes. In *Proceedings of the International Conference on Computer Vision (ICCV)*, 2023.
- [17] Jiahao Lu, Jiacheng Deng, Chuxin Wang, Jianfeng He, and Tianzhu Zhang. Query refinement transformer for 3d instance segmentation. In *Proceedings of the IEEE/CVF International Conference on Computer Vision (ICCV)*, pages 18516–18526, October 2023.
- [18] Damien Robert, Hugo Raguét, and Loïc Landrieu. Efficient 3d semantic segmentation with superpoint transformer. *Proceedings of the IEEE/CVF International Conference on Computer Vision*, 2023.

- [19] Damien Robert, Hugo Raguet, and Loic Landrieu. Scalable 3d panoptic segmentation as superpoint graph clustering. *Proceedings of the IEEE International Conference on 3D Vision*, 2024.
- [20] Salwa Al Khatib, Mohamed El Amine Boudjoghra, Jean Lahoud, and Fahad Shahbaz Khan. 3d instance segmentation via enhanced spatial and semantic supervision. In *Proceedings of the IEEE/CVF International Conference on Computer Vision (ICCV)*, pages 541–550, October 2023.
- [21] Christopher Choy, Jaesik Park, and Vladlen Koltun. Fully convolutional geometric features. In *Proceedings of the IEEE International Conference on Computer Vision*, pages 8958–8966, 2019.
- [22] Spconv Contributors. Spconv: Spatially sparse convolution library. <https://github.com/traveller59/spconv>, 2022.
- [23] Christopher Choy, Junha Lee, Rene Ranftl, Jaesik Park, and Vladlen Koltun. High-dimensional convolutional networks for geometric pattern recognition. In *Proceedings of the IEEE Conference on Computer Vision and Pattern Recognition*, 2020.
- [24] Gilles Puy, Spyros Gidaris, Alexandre Boulch, Oriane Siméoni, Corentin Sautier, Patrick Pérez, Andrei Bursuc, and Renaud Marlet. Three pillars improving vision foundation model distillation for lidar. In *CVPR*, 2024.
- [25] Songyou Peng, Kyle Genova, Chiyu "Max" Jiang, Andrea Tagliasacchi, Marc Pollefeys, and Thomas Funkhouser. Openscene: 3d scene understanding with open vocabularies. In *Proceedings of the IEEE/CVF Conference on Computer Vision and Pattern Recognition (CVPR)*, 2023.
- [26] Haoyu Guo, He Zhu, Sida Peng, Yuang Wang, Yujun Shen, Ruizhen Hu, and Xiaowei Zhou. Sam-guided graph cut for 3d instance segmentation. *arXiv preprint arXiv:2312.08372*, 2023.
- [27] Runyu Ding, Jihan Yang, Chuhui Xue, Wenqing Zhang, Song Bai, and Xiaojuan Qi. Lowis3d: Language-driven open-world instance-level 3d scene understanding, 2023.
- [28] Yining Hong, Haoyu Zhen, Peihao Chen, Shuhong Zheng, Yilun Du, Zhenfang Chen, and Chuang Gan. 3d-llm: Injecting the 3d world into large language models. *NeurIPS*, 2023.
- [29] Jiangyong Huang, Silong Yong, Xiaojian Ma, Xiongkun Linghu, Puhao Li, Yan Wang, Qing Li, Song-Chun Zhu, Baoxiong Jia, and Siyuan Huang. An embodied generalist agent in 3d world. In *Proceedings of the International Conference on Machine Learning (ICML)*, 2024.
- [30] Daichi Azuma, Taiki Miyانشi, Shuhei Kurita, and Motoaki Kawanabe. Scanqa: 3d question answering for spatial scene understanding. In *Proceedings of the IEEE/CVF Conference on Computer Vision and Pattern Recognition (CVPR)*, 2022.
- [31] Panos Achlioptas, Ahmed Abdelreheem, Fei Xia, Mohamed Elhoseiny, and Leonidas J. Guibas. ReferIt3D: Neural listeners for fine-grained 3d object identification in real-world scenes. In *16th European Conference on Computer Vision (ECCV)*, 2020.
- [32] Dave Zhenyu Chen, Angel X Chang, and Matthias Nießner. Scanrefer: 3d object localization in rgb-d scans using natural language. *16th European Conference on Computer Vision (ECCV)*, 2020.
- [33] Sijin Chen, Xin Chen, Chi Zhang, Mingsheng Li, Gang Yu, Hao Fei, Hongyuan Zhu, Jiayuan Fan, and Tao Chen. LI3da: Visual interactive instruction tuning for omni-3d understanding, reasoning, and planning, 2023.
- [34] Sijin Chen, Hongyuan Zhu, Xin Chen, Yinjie Lei, Gang Yu, and Tao Chen. End-to-end 3d dense captioning with vote2cap-detr. In *Proceedings of the IEEE/CVF Conference on Computer Vision and Pattern Recognition*, pages 11124–11133, 2023.
- [35] Zhenyu Chen, Ali Gholami, Matthias Nießner, and Angel X Chang. Scan2cap: Context-aware dense captioning in rgb-d scans. In *Proceedings of the IEEE/CVF Conference on Computer Vision and Pattern Recognition*, pages 3193–3203, 2021.
- [36] Heng Wang, Chaoyi Zhang, Jianhui Yu, and Weidong Cai. Spatiality-guided transformer for 3D dense captioning on point clouds. In *Proceedings of the Thirty-First International Joint Conference on Artificial Intelligence, IJCAI-22*, 2022.

- [37] Zhu Ziyu, Ma Xiaojian, Chen Yixin, Deng Zhidong, Huang Siyuan, and Li Qing. 3d-vista: Pre-trained transformer for 3d vision and text alignment. In *ICCV*, 2023.
- [38] Xiaojian Ma, Silong Yong, Zilong Zheng, Qing Li, Yitao Liang, Song-Chun Zhu, and Siyuan Huang. Sqa3d: Situated question answering in 3d scenes. In *International Conference on Learning Representations*, 2023.
- [39] Maria Parelli, Alexandros Delitzas, Nikolas Hars, Georgios Vlassis, Sotirios Anagnostidis, Gregor Bachmann, and Thomas Hofmann. Clip-guided vision-language pre-training for question answering in 3d scenes. In *Proceedings of the IEEE/CVF Conference on Computer Vision and Pattern Recognition*, pages 5606–5611, 2023.
- [40] Alexandros Delitzas, Maria Parelli, Nikolas Hars, Georgios Vlassis, Sotirios Anagnostidis, Gregor Bachmann, and Thomas Hofmann. Multi-clip: Contrastive vision-language pre-training for question answering tasks in 3d scenes. *arXiv preprint arXiv:2306.02329*, 2023.
- [41] Yanmin Wu, Xinhua Cheng, Renrui Zhang, Zesen Cheng, and Jian Zhang. Eda: Explicit text-decoupling and dense alignment for 3d visual grounding. In *Proceedings of the IEEE Conference on Computer Vision and Pattern Recognition (CVPR)*, 2023.
- [42] Kaiyu Yue, Bor-Chun Chen, Jonas Geiping, Hengduo Li, Tom Goldstein, and Ser-Nam Lim. Object Recognition as Next Token Prediction. In *Computer Vision and Pattern Recognition Conference (CVPR)*, 2024.
- [43] Alessandro Conti, Enrico Fini, Massimiliano Mancini, Paolo Rota, Yiming Wang, and Elisa Ricci. Vocabulary-free image classification, 2023.
- [44] Xinyu Huang, Yi-Jie Huang, Youcai Zhang, Weiwei Tian, Rui Feng, Yuejie Zhang, Yanchun Xie, Yaqian Li, and Lei Zhang. Open-set image tagging with multi-grained text supervision, 2023.
- [45] Lin Chuang, Jiang Yi, Qu Lizhen, Yuan Zehuan, and Cai Jianfei. Generative region-language pretraining for open-ended object detection. In *Proceedings of IEEE Conference on Computer Vision and Pattern Recognition (CVPR)*, 2024.
- [46] Haoxuan You, Haotian Zhang, Zhe Gan, Xianzhi Du, Bowen Zhang, Zirui Wang, Liangliang Cao, Shih-Fu Chang, and Yinfei Yang. Ferret: Refer and ground anything anywhere at any granularity. *arXiv preprint arXiv:2310.07704*, 2023.
- [47] Qihang Yu, Xiaohui Shen, and Liang-Chieh Chen. Towards open-ended visual recognition with large language model. In *arxiv: 2311.08400*, 2023.
- [48] Yuqian Yuan, Wentong Li, Jian Liu, Dongqi Tang, Xinjie Luo, Chi Qin, Lei Zhang, and Jianke Zhu. Osprey: Pixel understanding with visual instruction tuning, 2023.
- [49] Haotian Liu, Chunyuan Li, Qingyang Wu, and Yong Jae Lee. Visual instruction tuning. In *NeurIPS*, 2023.
- [50] Yuxin Fang, Wen Wang, Binhui Xie, Quan Sun, Ledell Wu, Xinggang Wang, Tiejun Huang, Xinlong Wang, and Yue Cao. Eva: Exploring the limits of masked visual representation learning at scale. In *Proceedings of the IEEE/CVF Conference on Computer Vision and Pattern Recognition*, pages 19358–19369, 2023.
- [51] Wenliang Dai, Junnan Li, Dongxu Li, Anthony Meng Huat Tiong, Junqi Zhao, Weisheng Wang, Boyang Li, Pascale Fung, and Steven Hoi. Instructblip: Towards general-purpose vision-language models with instruction tuning, 2023.
- [52] Tsung-Yi Lin, Michael Maire, Serge Belongie, James Hays, Pietro Perona, Deva Ramanan, Piotr Dollár, and C Lawrence Zitnick. Microsoft coco: Common objects in context. In *Computer Vision—ECCV 2014: 13th European Conference, Zurich, Switzerland, September 6-12, 2014, Proceedings, Part V 13*, pages 740–755. Springer, 2014.
- [53] Agrim Gupta, Piotr Dollar, and Ross Girshick. Lvis: A dataset for large vocabulary instance segmentation. In *Proceedings of the IEEE/CVF conference on computer vision and pattern recognition*, pages 5356–5364, 2019.
- [54] Bolei Zhou, Hang Zhao, Xavier Puig, Sanja Fidler, Adela Barriuso, and Antonio Torralba. Scene parsing through ade20k dataset. In *Proceedings of the IEEE conference on computer vision and pattern recognition*, pages 633–641, 2017.

- [55] Marius Cordts, Mohamed Omran, Sebastian Ramos, Timo Rehfeld, Markus Enzweiler, Rodrigo Benenson, Uwe Franke, Stefan Roth, and Bernt Schiele. The cityscapes dataset for semantic urban scene understanding. In *Proceedings of the IEEE conference on computer vision and pattern recognition*, pages 3213–3223, 2016.
- [56] Pitchaporn Rewatbowornwong, Nattanat Chatthee, Ekapol Chuangsuwanich, and Supasorn Suwajanakorn. Zero-guidance segmentation using zero segment labels. In *IEEE International Conference on Computer Vision (ICCV)*, 2023.
- [57] Jacob Devlin, Ming-Wei Chang, Kenton Lee, and Kristina Toutanova. Bert: Pre-training of deep bidirectional transformers for language understanding. *arXiv preprint arXiv:1810.04805*, 2018.
- [58] Nils Reimers and Iryna Gurevych. Making monolingual sentence embeddings multilingual using knowledge distillation. In *Proceedings of the 2020 Conference on Empirical Methods in Natural Language Processing*. Association for Computational Linguistics, 11 2020.
- [59] Xingyi Zhou, Rohit Girdhar, Armand Joulin, Philipp Krähenbühl, and Ishan Misra. Detecting twenty-thousand classes using image-level supervision. In *ECCV*, 2022.
- [60] Alexander Kirillov, Eric Mintun, Nikhila Ravi, Hanzi Mao, Chloe Rolland, Laura Gustafson, Tete Xiao, Spencer Whitehead, Alexander C. Berg, Wan-Yen Lo, Piotr Dollár, and Ross Girshick. Segment anything. *arXiv:2304.02643*, 2023.
- [61] Angela Dai, Angel X. Chang, Manolis Savva, Maciej Halber, Thomas Funkhouser, and Matthias Nießner. Scannet: Richly-annotated 3d reconstructions of indoor scenes. In *Proc. Computer Vision and Pattern Recognition (CVPR)*, IEEE, 2017.
- [62] Wei-Lin Chiang, Zhuohan Li, Zi Lin, Ying Sheng, Zhanghao Wu, Hao Zhang, Lianmin Zheng, Siyuan Zhuang, Yonghao Zhuang, Joseph E. Gonzalez, Ion Stoica, and Eric P. Xing. Vicuna: An open-source chatbot impressing gpt-4 with 90%* chatgpt quality, March 2023.
- [63] Tianhe Ren, Shilong Liu, Ailing Zeng, Jing Lin, Kunchang Li, He Cao, Jiayu Chen, Xinyu Huang, Yukang Chen, Feng Yan, et al. Grounded sam: Assembling open-world models for diverse visual tasks. *arXiv preprint arXiv:2401.14159*, 2024.